## Mixed-Mode Fracture. Curved Crack Path

A crack pre-exists in a body. When the body is loaded, the two faces of the crack may simultaneously open and slide relative to each other. The crack is said to be under a mixed-mode condition. When the load reaches a critical level, the crack starts to grow, and usually kinks into a new direction. Subsequently the crack often grows along a curved path.

This lecture discusses the critical condition to initiate the growth, the direction of the kink, and the method to predict the curved path.

Mixed-mode loading. We model the body by the linear elastic theory, and assume the material is homogeneous and isotropic. We further assume the small-scale yielding condition.   Consequently, in the body there exists an annulus, large compared to the inelastic zone around the front of the crack, but small compared to the length of the crack. Inside the annulus, the field of stress is predominantly described by the square-root singular field.

This singular field was discussed in the lecture on the stress intensity factor (http://imechanica.org/node/7579). The field is a linear combination of three fields, called mode I, mode II, and mode III field. Since that lecture, we have focused on cracks under the mode I condition. We now consider cracks under a combination of mode I and mode II loading. The body deforms under either the plane-strain or the plane-stress conditions.

Let (r,θ) be the polar coordinates centered at the tip of the crack.   The two faces of the crack coincide with the planes $\theta = +\pi$ and $\theta = -\pi$. The singular stress field is a linear combination of fields of the two modes, namely,
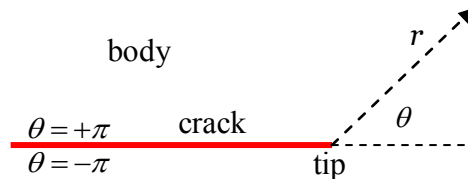
$$\sigma_{ij}(r,\theta) = \frac{K_I}{\sqrt{2\pi r}}\Sigma_{ij}^I(\theta) + \frac{K_{II}}{\sqrt{2\pi r}}\Sigma_{ij}^{II}(\theta).$$

The stress intensity factors, K_I and K_{II}, represent the amplitudes of opening and shearing loads, respectively. The field is square-root singular in r. The θ-dependent functions, $\Sigma_{ij}^I(\theta)$ and $\Sigma_{ij}^{II}(\theta)$, are given below.

The mode I field is symmetric with respect to the plane of the crack, so that $\Sigma_{r\theta}^I(0) = 0$. By convention, we set $\Sigma_{\theta\theta}^I(0) = 1$, such that the normal stress a distance r ahead the tip of the crack is

$$\sigma_{\theta\theta}(r,0) = \frac{K_I}{\sqrt{2\pi r}}.$$

This convention defines the stress intensity factor K_I. The angular distributions of the mode I field are

$$\Sigma_{rr}^I(\theta) = \cos\left(\frac{\theta}{2}\right)\left(1 + \sin^2\left(\frac{\theta}{2}\right)\right),$$

$$\Sigma_{\theta\theta}^I(\theta) = \cos^3\left(\frac{\theta}{2}\right),$$

$$\Sigma_{r\theta}^I(\theta) = \sin\left(\frac{\theta}{2}\right)\cos^2\left(\frac{\theta}{2}\right).$$

The mode II field is antisymmetric with respect to the plane of the crack, so that $\Sigma_{\theta\theta}^{II}(0)=0$. By convention, we set $\Sigma_{r\theta}^{II}(0)=1$, such that the shearing stress a distance r ahead the tip of the crack is

$$\sigma_{r\theta}(r,0)=\frac{K_{II}}{\sqrt{2\pi r}}\ .$$

This convention defines the stress intensity factor K_{II}. The angular distributions of the mode II field are

$$\Sigma_{rr}^{II}(\theta)=\sin\left(\frac{\theta}{2}\right)\left(1-3\sin^2\left(\frac{\theta}{2}\right)\right),$$

$$\Sigma_{\theta\theta}^{II}(\theta)=-3\sin\left(\frac{\theta}{2}\right)\cos^2\left(\frac{\theta}{2}\right),$$

$$\Sigma_{r\theta}^{II}(\theta)=\cos\left(\frac{\theta}{2}\right)\left(1-3\sin^2\left(\frac{\theta}{2}\right)\right).$$

Calculate stress intensity factors. Once a crack configuration is given, the stress intensity factors K_I and K_{II} are determined by solving the elasticity boundary value problem. For example, for a crack, length $2a$, in an infinite sheet subject to remote tensile stress σ and shearing stress τ, the stress intensity factors are

$$K_I=\sigma\sqrt{\pi a}\ ,$$

$$K_{II}=\tau\sqrt{\pi a}\ .$$

As a second example, consider a crack, length $2a$, in a large sheet. Remote from the crack, the sheet is under a tensile stress acting in the direction at angle β from the crack. The stress intensity factors are

$$K_I=\sigma\sqrt{\pi a}\sin^2\beta\ ,$$

$$K_{II}=\sigma\sqrt{\pi a}\sin\beta\cos\beta\ .$$

Solutions for many configurations of cracks have been collected in handbooks. Finite element methods have been used to determine the stress intensity factors under the mixed-mode conditions.
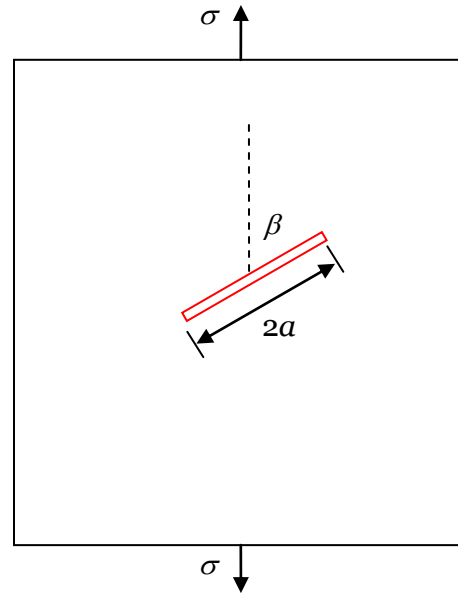
Energy release rate. The energy release rate G is still defined as the reduction of the potential energy associated with the extension of the crack by a unit area. The energy release rate relates to the two stress intensity factors by (Irwin, 1957)

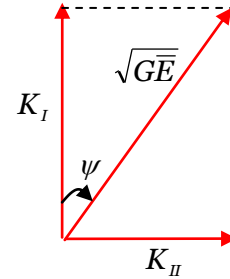$$G=\frac{1}{\overline{E}}\left(K_I^2+K_{II}^2\right).$$

Mode angle. The relative amount of mode II to mode I is specified by the mode angle ψ defined by

$$\tan\psi = K_{II}/K_I.$$

We will be interested in situations that the crack front is under tension, rather than compression, namely, $K_I \geq 0$. The mode angle is restricted in the range

$$-\pi/2 \leq \psi \leq \pi/2.$$

A pure mode I crack corresponds to $\psi = 0$, while a pure mode II crack corresponds to either $\psi = +\pi/2$ or $\psi = -\pi/2$.

Instead of using K_I and K_{II} to represent the external loads, we often use G to represent the amplitude of the loads, and use ψ to represent the mode of the loads.

Critical condition to initiate the growth of a crack under mixed-mode loading. Consider a pre-existing crack subject to mixed-mode loading. We assume the small-scale yielding condition, such that an annulus exists, within which the stress field is predominantly given by the square-root singular field. The field is fully represented by the two parameters, K_I and K_{II}. That is, the two stress intensity factors represent the external boundary conditions. The two "messengers" transmit the external boundary conditions to the crack tip.

In the (K_I, K_{II}) plane, each point represents a loading condition. The critical condition for the onset of the growth of the crack is represented by the curve on the (K_I, K_{II}) plane. This curve may be determined experimentally. For this curve to be useful, one should ascertain that the curve is independent of type of specimen and length of the pre-existing crack.

The critical condition can also be represented on the (G, ψ)-plane.
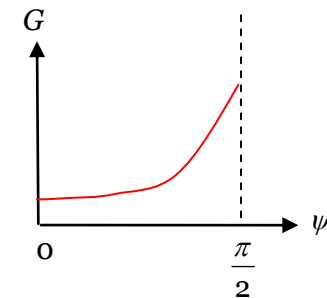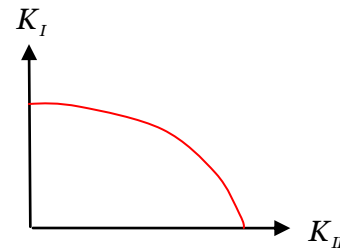
Direction of the kink. Under a mixed-mode condition, upon initiating, a planar crack often kinks at an angle from its original plane. The direction of the kink depends on the relative amount of mode II to mode I load. Erdogan and Sih (1963) showed that the experimentally measured direction of the kink in plexiglass is well predicted by the criterion that the crack kinks to the plane with the maximum hoop stress.

For the stationary crack, the hoop stress near the crack tip is

$$\sigma_{\theta\theta}(r,\theta) = \frac{K_I}{\sqrt{2\pi r}}\cos^3\left(\frac{\theta}{2}\right) - \frac{K_{II}}{\sqrt{2\pi r}}3\cos^2\left(\frac{\theta}{2}\right)\sin\left(\frac{\theta}{2}\right).$$

The hoop stress maximizes at an angle θ^*, given by

$$\tan\left(\frac{\theta^*}{2}\right) = -\frac{2K_{II}/K_I}{1+\sqrt{1+8(K_{II}/K_I)^2}}.$$

We will only consider an opening crack, so that $K_I > 0$. When $K_{II} > 0$, the crack kinks down (i.e., $\theta^* < 0$). When $K_{II} < 0$, the crack kinks down. When the crack is pure mode I, this criterion predicts that the crack extends straight ahead. When the crack is pure mode II, this criterion predicts that the crack kinks at an angle $\theta^* = 70.5°$.

A crack grows along a mode I path. In a body subject to general loading, a crack may grow along a curved path. Existing observations seem to support the following hypothesis. In a homogenous, isotropic, and linearly elastic material, a crack seeks a path such that the tip of the crack is locally under the mode I condition.

For example, use scissors to cut a short crack in a piece of paper, at an acute angle from the edge of the paper. When the paper is pulled, the crack grows into the direction perpendicular to the pulling force.

As a second example, it is well known that a crack in a double-cantilever beam is unstable: the crack tends to curve one way or the other. By symmetry, the crack on the mid-plane of the sample is pure mode I. This mode I path, however, is unstable. A crack, lying slightly off the mid-plane, has a mode II component that tends to deflect the crack further away from the mid-plane.

A crack growing in a substrate beneath an adherent film. Thouless et al. (1987). Consider a thin film well bonded to the substrate, and is under a residual tensile stress. It is sometimes observed that a crack starts from the edge of the film, dives into the substrate, and then grows parallel to the interface. In the crack wake, the residual stress in the film is partially relieved, and the film and a thin layer of the substrate material underneath form a composite plate, bending up.

This observation may seem to be peculiar. Were the crack to run on the film-substrate interface, the residual stress in the film would be fully relieved in the wake of the crack. However, such a global energy consideration has no physical basis: it is the local process of bond breaking that selects the crack path. The experimental observation has been interpreted that the crack grows along a mode I path.
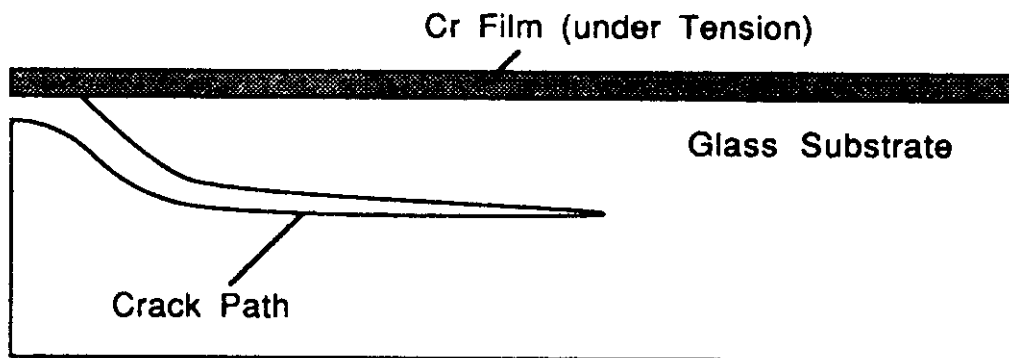
To see how this works, consider a special case that the thin film and the substrate have similar elastic modulus. Let h be the thickness of the film, and d be the depth of the crack parallel to the interface. When the crack is long compared to d, the effect of the residual stress on the crack is well described by the equivalent axial force and bending moment:

$$P = \sigma h, M = \frac{1}{2}\sigma h(d - h).$$

To select the crack path, we need to determine the stress intensity factors.

The energy release rate can be readily calculated by using elementary considerations, giving

$$G = \frac{P^2}{2\bar{E}d} + \frac{6M^2}{\bar{E}d^3}.$$

Recall Irwin's relation between the energy release rate and the stress intensity factors:

$$G = \frac{K_I^2}{\bar{E}} + \frac{K_{II}^2}{\bar{E}}.$$

Linearity and dimensional considerations dictate that the stress intensity factors related to the axial force and the moment as

$$K_I = aPd^{-1/2} + bMd^{-3/2}$$

$$K_{II} = mPd^{-1/2} + nMd^{-3/2}$$

A comparison of the two expressions of the energy release rate gives that

$$a^2 + m^2 = \frac{1}{2}, \; b^2 + n^2 = 6, \; an + bm = 0$$

These are three algebraic equations among four numbers, so that only one number is undetermined. The three equations are satisfied by

$$a = \frac{1}{\sqrt{2}}\cos\omega, \; m = \frac{1}{\sqrt{2}}\sin\omega, \; b = \sqrt{6}\sin\omega, \; n = -\sqrt{6}\cos\omega$$

In terms of ω, the stress intensity factors are given by

$$K_I = \frac{1}{\sqrt{2}}\left(Pd^{-1/2}\cos\omega + 2\sqrt{3}Md^{-3/2}\sin\omega\right),$$

$$K_{II} = \frac{1}{\sqrt{2}}\left(Pd^{-1/2}\sin\omega - 2\sqrt{3}Md^{-3/2}\cos\omega\right).$$

The angle ω cannot be calculated by elementary considerations. It requires a numerical solution of the boundary-value problem. The solution gives

$$\omega \approx 52^\circ.$$

Suppose that the crack selects the depth d^* by the condition that $K_{II} = 0$, and we obtain that

$$d^* = 3.8h.$$

One can further confirm that the mode I path is stable in that, if a parallel crack at a depth d different from d^*, then K_{II} is nonzero and is in the direction that tends to deflect the crack back toward the depth d^*.

Extended finite element method (XFEM). Curved crack paths can be simulated using numerical methods. For a given crack configuration, one solves the elasticity boundary value problem, and computes the stress intensity factors K_I and K_{II}. One then advances the crack by a small length in the direction, say, set by the criterion of maximum hoop stress. The path so selected should be essentially a mode I path.

The regular finite element method meshes the geometry of the crack and uses a fine mesh near the crack tip. When the crack grows, remeshing is required. To circumvent these difficulties, an extended finite element method (XFEM) has

been advanced. For the nodes around the crack tip, one adds enriching functions derived from the singular crack-tip stress field. For nodes on the crack faces, one adds the Heaviside function to represent the displacement jump. Consequently, the mesh can be coarse near the crack tip, and the elements need not to conform to the crack geometry. As the cracks grow, one updates the nodes to be enriched. No remeshing is necessary. See Moes, Dolbow and Belytschko (1999).

Mud crack in a thin film bonded to a substrate. For a single crack tip, the precise length for each increment is unimportant, so long as it is much smaller than the representative size of the sample. To simulate simultaneous growth of multiple cracks, however, one has to know how much to advance each crack. An ingredient of time-dependence has to be introduced into the model. For example, if the solid is susceptible to subcritical cracking, the V-G relation provides the needed information. Once the energy release rate is calculated for every crack tip in a given configuration, one advances each crack according to the kinetic law for a small time step. Similar ideas apply to fatigue cracks growing in a metal under cyclic loads.

Similarly, one can simulate the growth of a crack in three dimensions with a curved front by advancing each point on the crack front according to the kinetic law and its local energy release rate. Because the crack extends under the mode I conditions, the V-G curve can be obtained experimentally using a specimen containing a single straight mode I crack.
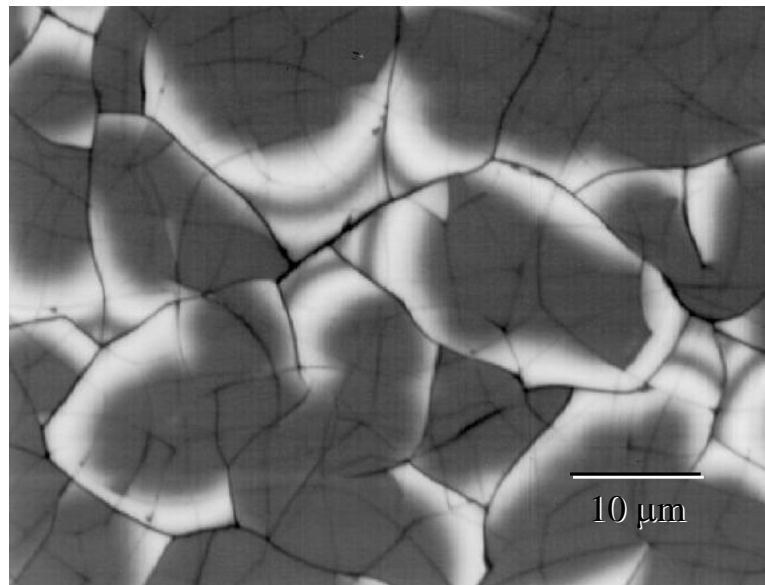
Cracked SiN film of about 1 um thick, grown on silicon substrate. The contrast also indicates that the film was partially debonded. Courtesy of Dr. Qing Ma, of Intel Coorporation.
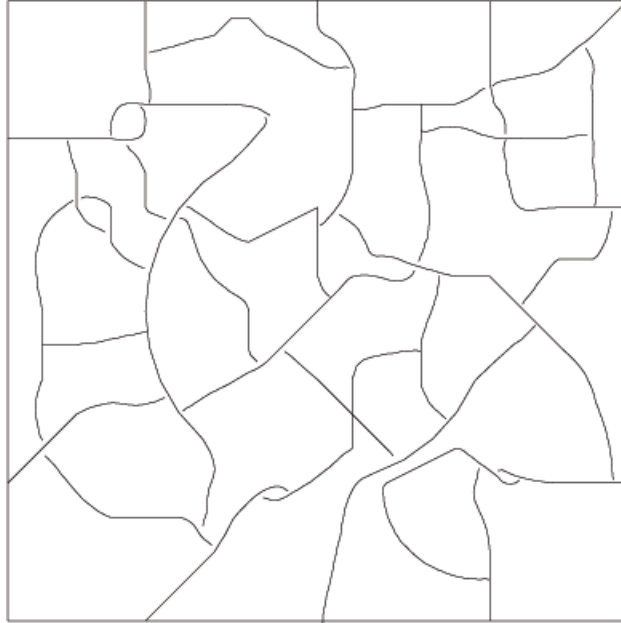
Simulation using XFEM (Liang, et al., 2003).

Crack path in a compliant layer sandwiched between two stiff substrates. (Chai, 1987; Pease et al., 2007). Describe the experimental observation.
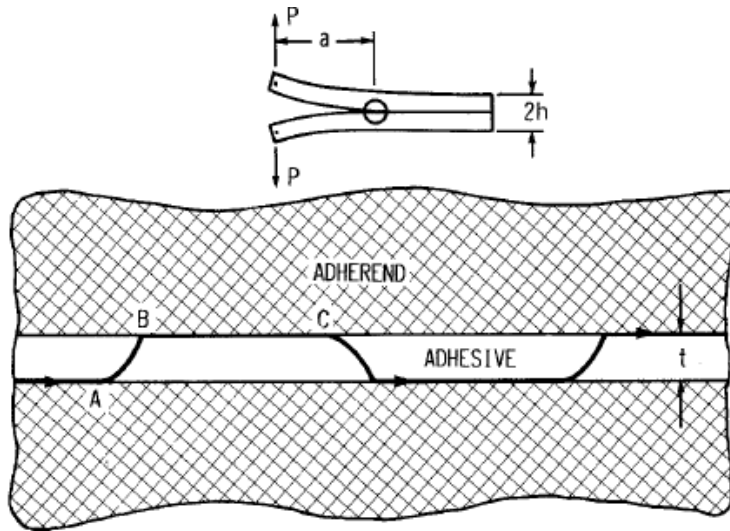

Figure 1. Crack trajectory (heavy line) in a DCB adhesive joint fracture specimen. The lower part is a magnified view of the circled area in the upper part.
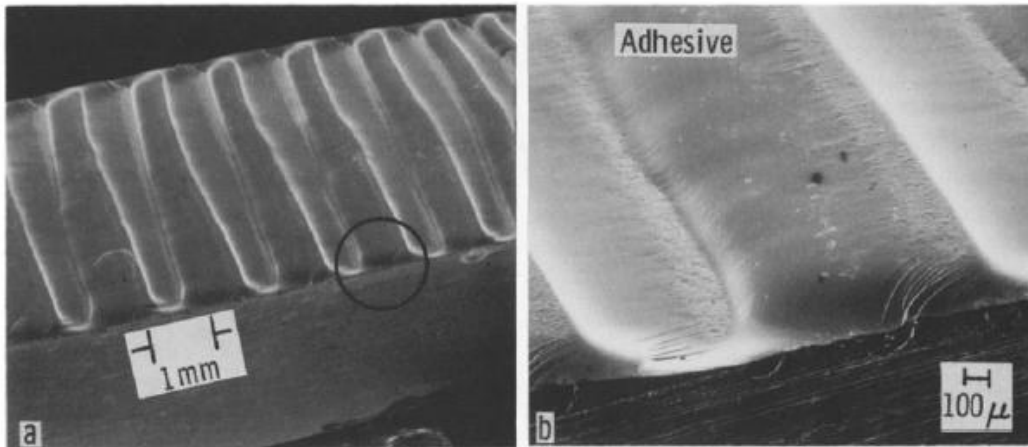

Figure 2. Alternating crack trajectory observed in testing of adhesive joint specimen at two magnifications. Growth is from left to right. Adhesive is Narmco 5208, a brittle epoxy. Adherend is aluminum. $t = 0.25$ mm, $h = 6.3$ mm.

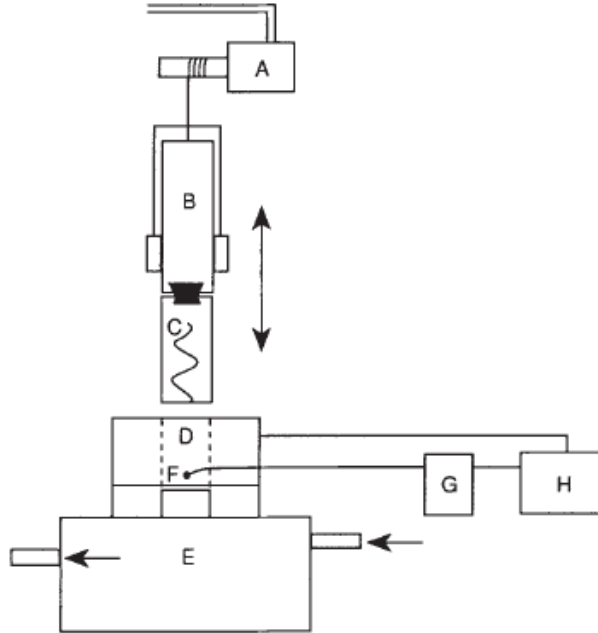**Crack path in a quenched glass plate.** (Yuse and Sano, 1993; Yang and Ravi-Chandar, 2001)

FIG. 1 Experimental arrangement. D is a heater (controlled to an accuracy of ±0.2 K) consisting of an aluminium block with a slot of depth 0.6 mm. E is a cooled water bath (controlled to an accuracy of ±0.1 K). The temperature difference between them is typically 70 K and the separation is 10.5 ± 0.5 mm. The glass plate (C) is attached to the linear slide (B), which is suspended on a stainless steel wire wound on a brass cyinder driven by the computer-controlled stepping motor (A). F is a temperature sensor, G and H are temperature controllers.
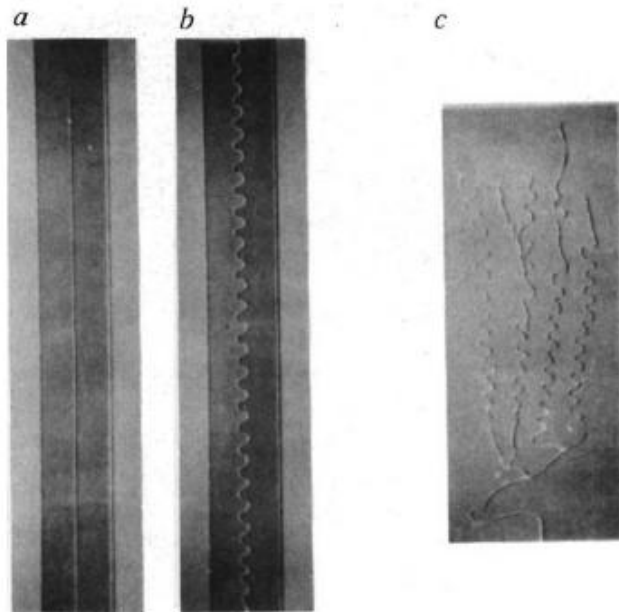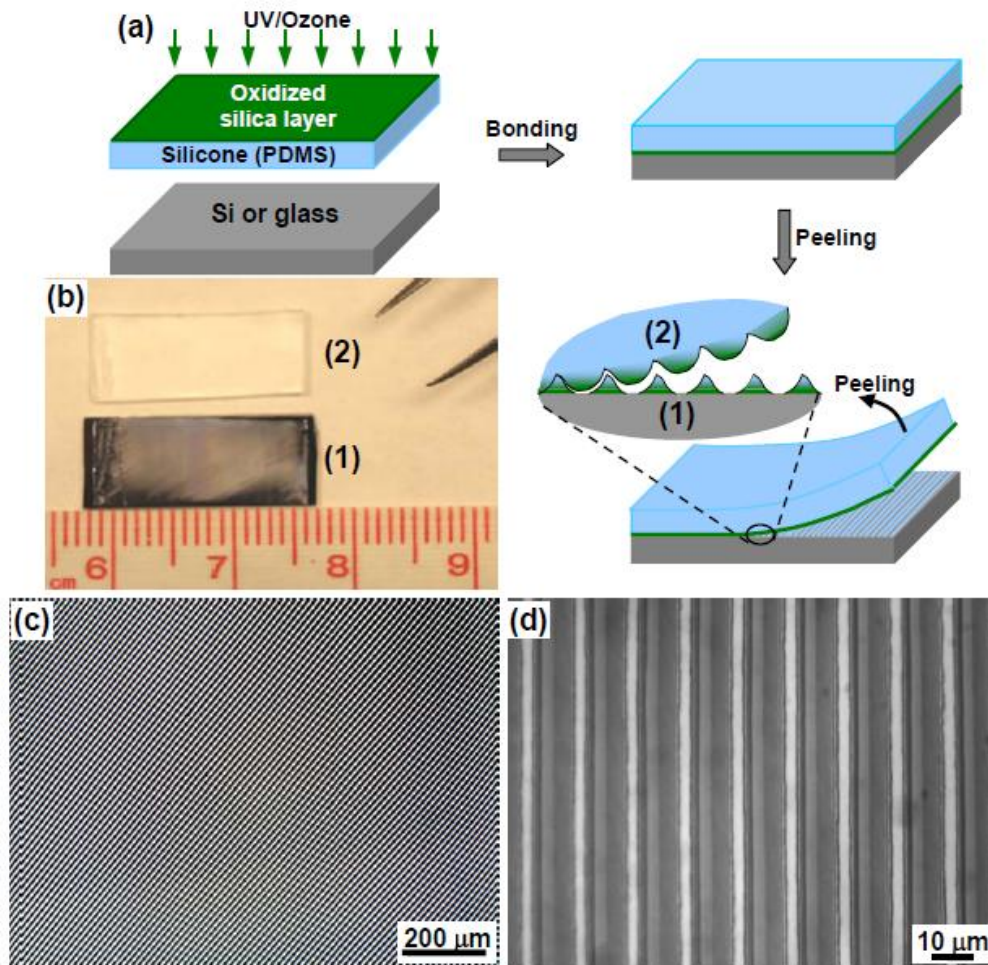

FIG. 2 Typical examples of three different types of cracks: a, a straight crack, b, oscillating crack, c, branched crack. Sample size (a and b) $10 \times 100 \times 0.11$ mm^3, (c) $24 \times 60 \times 0.13$ mm^3.

Formation of strips during pealing an elastomer from a glass substrate. (Cai and Zhang Newby, 2010)

(a) The schematic procedure for fabricating silicone strips by peeling: (i) UV/Ozone treatment of the silicone sheet and the substrate (silicon wafer or glass); (ii) Bonding of the silicone sheet and the substrate upon annealing at 100˚C for 40 min. (iii) Peeling the silicone sheet away from the substrate with the enlarged peeling front showing both adhesive and cohesive failure occur, leading two complementary patterns (1 and 2). (b) A photograph showing the fabricated patterns (1 and 2) at a centimeter scale. (c) A representative optical microscopic image of the strips on the substrate. (c) A high-magnification image of (c).

Mixed-mode fracture in soft materials. Less work is available. See Hocine and Abdelaziz (2009), W.-C. Lin et al. (2009), Shergold and Fleck (2005).

References

H. Chai, A note on crack trajectory in an elastic strip bounded by rigid substrates. International Journal of Fracture 32, 211-213 (1987).
Y.G. Cai and B.M. Zhang Newby, Fracture-induced formation of parallel silicone strips. Journal of Materials Research. In press. **DOI:** 10.1557/JMR.2010.0106

F. Erdogan and G.C. Sih, On the crack extension in plates under plane loading and transverse shear. Journal of Basic Engineering 85, 519-527 (1963).

N.A. Hocine and M.N. Abdelaziz, Fracture analysis of rubber-like materials using global and local approaches: Initiation and propagation direction of a crack.

W.C. Lin, K.J. Otim, J.L. Lenhart, P.J. Cole, and K.R. Shull, Indentation fracture of silicone gels. Journal of Materials Research 24, 957-965 (2009).

M.D. Thouless, A.G. Evans, M.F. Ashby, J.W. Hutchinson. The edge cracking and spalling of brittle plates. Acta Met. 35, 1333-1341 (1987). http://www.seas.harvard.edu/hutchinson/papers/386.pdf

J. Liang, R. Huang, J.H. Prévost, and Z. Suo, Evolving crack patterns in thin films with the extended finite element method. International Journal of Solids and Structures 40, 2343-2354 (2003). http://www.deas.harvard.edu/suo/papers/137.pdf

N. Moes, J. Dolbow and T. Belytschko, A finite element method for crack growth without remeshing. International Journal for Numerical Methods in Engineering 46, 131-150 (1999).

L.F. Pease, P. Deshpande, Y. Wang, W.B. Russel, and S.Y. Chou, Self-formation of sub-60-nm half-pitch gratings with large areas through fracturing. Nature Nanotechnology 2, 545-548 (2007).

O.A. Shergold and N.A. Fleck, Experimental investigation into deep penetration of soft solids by sharp and blunt punches, with application to the piercing of skin. Journal of Biomedical Engineering 127, 838-848 (2005).

B. Yang and K. Ravi-Chandar, Crack path instabilities in a quenched glass plate. Journal of the Mechanics and Physics of Solids 49, 91-130 (2001).

A. Yuse and M. Sano, Transition between crack patterns in quenched glass plates. Nature 362, 329-331 (1993).